PROCEEDINGS, 42nd Workshop on Geothermal Reservoir Engineering
Stanford University, Stanford, California, February 13-15, 2017
SGP-TR-212

Modeling the Hydraulic Fracture Stimulation performed for Reservoir Permeability Enhancement at the Grimsel Test Site, Switzerland

D. Vogler, R.R. Settgast, C.S. Sherman, V.S. Gischig, R. Jalali, J.A. Doetsch, B. Valley, K.F. Evans, F. Amann and M.O. Saar

ETH Zurich, Zurich, Switzerland.

davogler@ethz.ch

Keywords: EGS, Hydraulic Fracturing, Microseismicity, Reservoir Stimulation, Numerical Modeling

ABSTRACT

In-situ hydraulic fracturing has been performed on the decameter scale in the Deep Underground rock Laboratory (DUG Lab) at the Grimsel Test Site (GTS) in Switzerland in order to measure the minimum principal stress magnitude and orientation. Conducted tests were performed in a number of boreholes, with 3–4 packer intervals in each borehole subjected to repeated injection. During each test, fluid injection pressure, injection flow rate and microseismic events were recorded amongst others. Fully coupled 3D simulations have been performed with the LLNL's GEOS simulation framework. The methods applied in the simulation of the experiments address physical processes such as rock deformation/stress, LEFM fracture mechanics, fluid flow in the fracture and matrix, and the generation of micro-seismic events. This allows to estimate the distance of fracture penetration during the injection phase and correlate the simulated injection pressure with experimental data during injection, as well as post shut-in. Additionally, the extent of the fracture resulting from simulations of fracture propagation and microseismic events are compared with the spatial distribution of the microseismic events recorded in the experiment.

1. INTRODUCTION

Oil, gas and geothermal reservoirs rely on sufficiently high reservoir permeability to achieve target production rates. However, Enhanced Geothermal Systems (EGS) have the potential for providing sustainable energy production from geothermal heat sources at great depths, even though the formation originally has a low permeability and has little water in place (Tester et al. 2006). The permeability is increased through hydraulic stimulation treatments in which large fluid volumes are injected. Such high-pressure fluid injections can drive tensile hydraulic fractures into the target formation (Economides et al. 2000, McClure & Horne 2014a,b, Detournay 2016) and also result in the activation in shear of pre-existing, critically stressed fractures or fault zones (hydro-shearing) (Evans et al. 1999, Evans 2005a). Hydraulic fracturing and hydro-shearing can thereby be used to achieve the fracture permeabilities required to obtain sufficiently high fluid circulation and corresponding heat extraction (Evans 2005a , Evans et al. 2005b, Gischig & Wiemer 2013, Guo et al. 2016, Vogler et al. 2016b). Both mechanisms commonly generate microseismicity, which constitutes an essential tool for mapping the migration of pressure and flow within the rock mass during reservoir creation (e.g. Niitsuma et al, 1999, Wolhart et al. 2006, Kim 2013, Deichmann et al. 2014, McClure & Horne 2014b). When large fluid volumes are injected, significant earthquakes may be induced, which can lead to the termination of reservoir operations (Kim 2013, Kraft & Deichmann 2014). Within the context of this paper, microseismic signals observed during minifrac stress measurements can indicate the dimension and propagation direction of the induced hydraulic fractures, which can be used to determine the direction of the minimum principal stress.

This study focuses on numerical simulations of hydraulic fracture propagation and attendant microseismicity during minifrac stress tests conducted in the Deep Underground Geothermal Laboratory (DUG Lab) at the Grimsel Test Site, Switzerland (Gischig et al. 2017). Simulations of hydraulic fracture dimensions, as indicated by the propagation of discrete fractures and the occurrence of microseismic events, are scrutinized with respect to the in-situ datasets.

Figure 1: Location of the Deep Underground rock Laboratory at the Grimsel Test Site (GTS) in the Swiss Alps.

METHODS

An experiment is underway at the Grimsel Test Site (GTS), in the Swiss Alps (Figure 1, Gischig et al. (2017)) that is intended to advance our understanding of the fundamental processes activated when stimulating Enhanced Geothermal Systems (EGS). The GTS is operated by the Swiss National Cooperative for the Disposal of Radioactive Waste (Nagra) as a centre for underground research and development. The GTS is located in the granitic formations of the Aar Massif, about 1730 meters above sea-level and 450 meters beneath the Juchlistock (ground surface). The total tunnel length in the laboratory is about 1 km and the total length of cored boreholes is above 5 km. The experiments conducted at the GTS aim to advance; (i) quantitative capabilities to model stimulation and reservoir operation, (ii) process understanding and validation in underground lab experiments, and (iii) develop a petrothermal (i.e., EGS) Pilot and Demonstration (P&D) project.

As part of the initial rock mass characterization, a number of small-scale hydraulic fractures (mini-fracs) were initiated and propagated in order to measure the in-situ minimum principal stress magnitude and orientation. Three to four packed-off intervals in three boreholes (Figure 2a) were each subjected to fluid injection until breakdown and fracture propagation were observed. During testing, the experimental rock volume was geophysically monitored (Figures 2b and d). The present study focuses on the injection cycles of mini-fracs performed at 18 m (SB3-18) and 8 m depth (SB3-8) along sub-horizontal borehole SB3. At these borehole locations, three fracture reopening injection cycles (injection cycles 2-4) were performed after an initial breakdown cycle (injection cycle 1). The fluid volumes injected during cycles 1-4 into intervals SB3-18 and SB3-8 were 0.5, 1.6, 2.5, 3.3 litres (7.9 litres total) and 1.1, 1.8, 3.3, 4.2 litres (10.4 litres total) respectively. An example for a breakdown cycle and subsequent refrac cycles for borehole SB3 at 8 m depth is given in Figure 3. During one injection cycle, the fracture propagates until fluid injection is stopped and the wellbore is shut-in to determine the pressure decline curve. The wellbore is then opened and part of the injected fluid is recovered.

The GTS is excavated in Granite and Granodiorite and has hosted numerous diverse studies relevant to the current project. Mechanical and hydraulic properties not determined during the present experiments were obtained from previous studies (Keusen et al. 1989, Pahl et al. 1989, Konietzky 1995). The principal stress magnitudes in the borehole derived from over-coring measurements conducted in the current program were estimated to be σ_1 = 17.3, σ_2 = 9.7 and σ_3 = 8.3 MPa (Figure 2c, Gischig et al. 2017). It is noteworthy, that σ_3 is roughly parallel to borehole SB3.

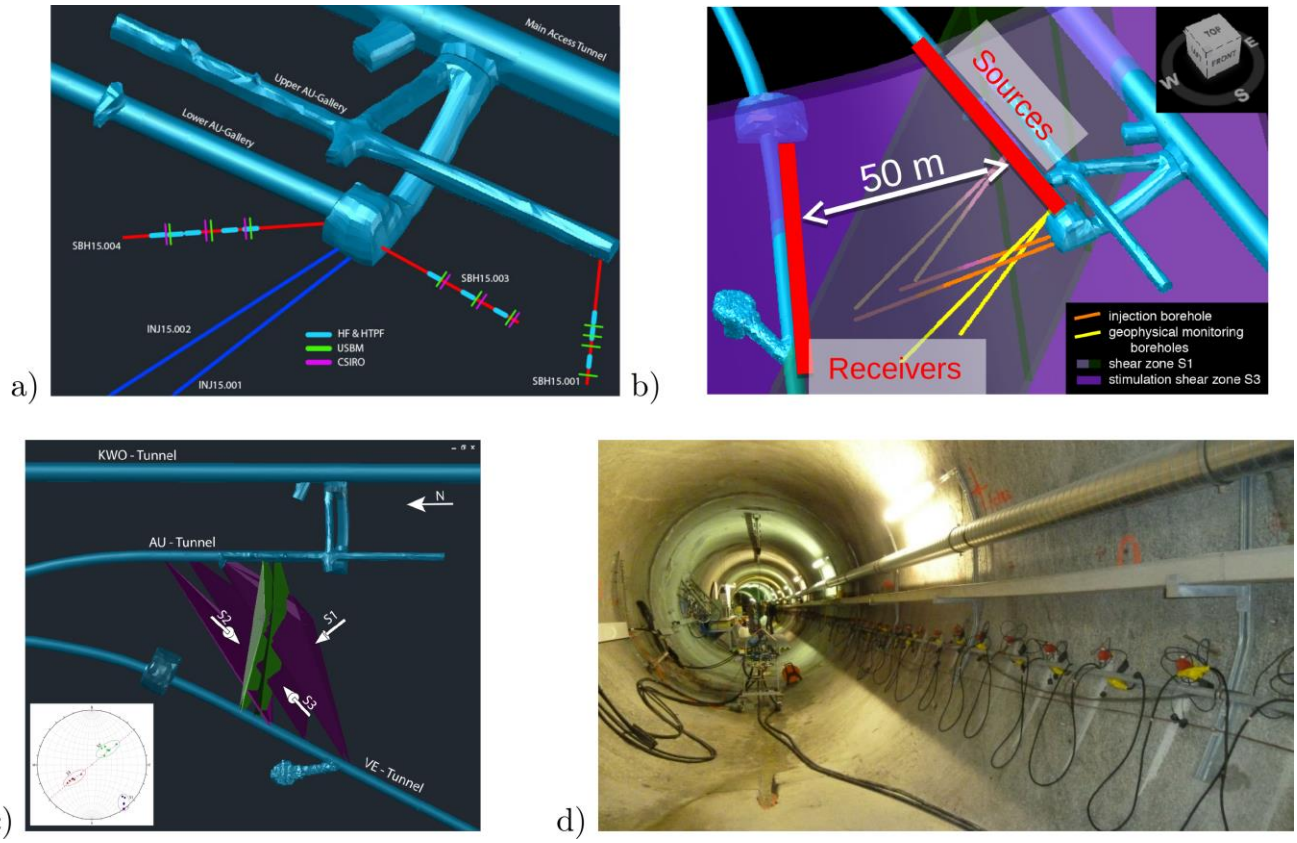

Figure 2: GTS - a) Borehole locations; b) Monitoring of fault zones; c) Main fault zones and principal stress orientations; d) Tunnel view.

The numerical simulator GEOS, developed at Lawrence Livermore National Laboratory (Settgast et al. 2014, 2016), is used to simulate the injection phases. GEOS is a massively parallel multi-physics framework, which incorporates capabilities to model hydraulic fracturing (Settgast et al. 2012, 2014, Fu et al. 2015, Settgast et al. 2016); seismic events (Sherman et al. 2016); fracture shearing (Annavarapu et al. 2015); thermal drawdown (Fu et al. 2016); matrix flow and heat transport (Guo et al. 2016); flow in rough fractures (Vogler et al. 2016a); geochemical transport and reaction (Walsh et al. 2012, 2013); and simulations of immiscible fluid flow (Walsh & Carroll 2013). The numerical solver employed in this study offers fully coupled hydro-mechanics (HM) and implicit time stepping. Solid body deformation is modeled with a finite element method and fluid flow in fractures and the matrix is modeled with a finite volume method. Fracture propagation employs an energy-based fracture mechanics concept, fluid flow in the fracture is based on lubrication theory and fluid leak-off uses Carter's leak-off method. In this study, the fracture is initiated with a notch in the location of the packer interval. A detailed explanation of the GEOS framework can be found in Settgast et al. (Settgast et al. 2016).

Modeling of microseismic events in GEOS can be performed with a full mechanical treatment or with a point-source approximation (Sherman et al. 2016). In this study, the point-source approximation is used. Joint sets are characterized by statistical distributions of location, dimension, orientation and material properties, and are mapped onto the finite element mesh. During the simulation, the stress state and fluid pressure are evaluated to determine local failure according to a Coulomb friction model. If an element fails, shear slip, dilation and the moment tensor of microseismic events are computed. Pressure loss between the pump setup in the GTS tunnel and the fracture are computed with an analytical wellbore solver, which incorporates frictional losses based on borehole dimensions, fluid entry into the fracture and near wellbore effects (such as fracture tortuosity near the wellbore). The wellbore solver is coupled to the fracture at the fracture entry. The flow rates injected into the reservoir during the experiment are applied to the head of the wellbore solver.

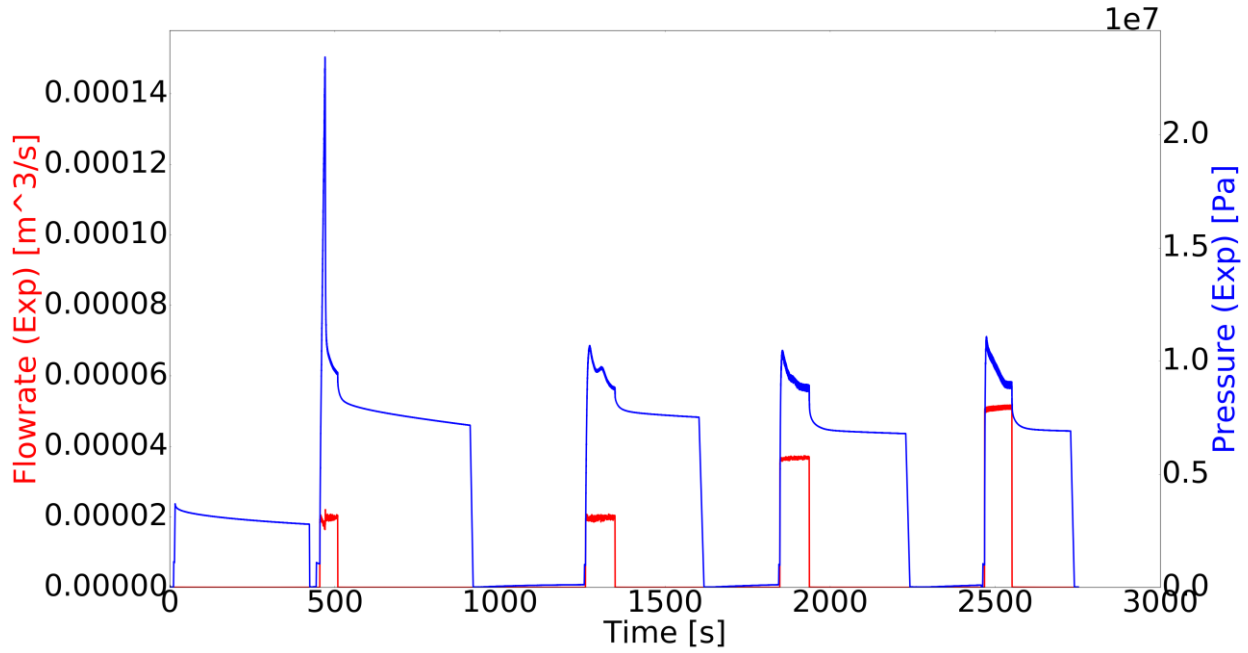

Figure 3: SB3-8. Example of injection cycles with fluid flow rate and pressure response in borehole SB3 at 8m depth.

RESULTS AND DISCUSSION

This section compares the results of the minifrac tests and numerical simulations, with a special emphasis on dimensions of the propagated fractures, the location and number of induced microseismic events, and the wellhead pressure response to the injected flow rates.

Simulation results for the fracture aperture field and pore pressure in and around the propagating fracture before shut-in are shown for four injection cycles (Figure 4). As σ_3 is roughly parallel to borehole SB3, Figure 4 shows fracture propagation is in a plane normal to the wellbore. The microseismic cloud recorded in the experiments, however, is not perfectly normal to the current best estimate of the minimal principal stress orientation, an observation which will be further discussed at the end of this section. The corresponding dimensions of the fracture after the four injection cycles are shown in Figures 5a-b. Here, fracture growth increases from about 4 m after the breakdown cycle, to 7.5 m (SB3-18, 7.9 litres injected) and 8.3 m (SB3-8, 10.4 litres injected) after the last injection cycle. Simulations of the pressure response at the wellhead during injection cycle 4 (SB3-8) are compared to the experiment in Figure 6. The rapid pressure decline after shut-in was only captured by employing the wellbore solver in the simulations. Without accounting for wellbore effects (mostly consisting of fracture entry losses), the simulated pressure decrease after shut-in was about 20% of the decrease computed by incorporating pressure losses between the pump setup and the fracture. As the intact rock at the GTS has a low porosity and permeability, fluid pressure only slowly diffuses away from the fracture and the fracture closes slowly. Optical televiewer data and other geophysical observations in SB3 suggest that the rock mass around the test interval probably contains a significant number of discontinuities at various scales. Additionally, the Granodiorite at the GTS can display strong foliation. These factors could conceivably influence the pressure response during injection, the fracture propagation direction and pressure diffusion after shut-in, and thus need to be further investigated. For example, smaller, unmapped fractures or flaws in the vicinity of the propagating fracture could cause the fluid to diffuse away from the fracture faster. The observed foliation of the rock mass in the GTS could influence the direction of fracture propagation as fracture toughness is likely to be anisotropic, although it is clear that the microseismic structures do not lie in the plane of the foliation (Gischig et al, 2017).

Experimental and simulation results for the microseismic activity around the propagating fracture in SB3-18 are shown in Figure 7. Here, the microseismic activity is viewed normal to the propagating fracture plane (i.e. horizontal view from the north). While the boundaries of the microseismic activity in the field experiment is more irregular, both experiment and simulation predict hydraulic fracture dimensions of around 7 m diameter after the last injection cycle. Triggered seismicity is more evenly distributed across all injection cycles in the simulations, the experimental data showing fewer seismic events during the first injection cycles. The propagation of simulated microseismic activity with the evolving fracture fluid pressure field around the fracture is shown in the snapshots of Figure 8. It should be noted that each snapshot shows the microseismic events that occur between the beginning of the respective injection cycle and the start of the next cycle, since a few events in the experiment occurred during shut-in. For injection cycle 4, Figure 8.4 shows pore pressure and seismic events up to the start of injection in the next packer interval (SB3-13), which occurred a few hours after the last injection cycle in SB3-18. This longer time period after injection cycle 4 causes an apparent smearing of the pressure front when compared to cycles 1-3.

As noted earlier, it proved difficult to reproduce the pressure decrease that occurred after shut-in. In the simulations, this was modeled with a number of effects in and near the wellbore, among which entrance losses at the fracture were most significant. However, further study of the system behavior after shut-in is required. Heterogeneity and anisotropy of the rock mass are likely to influence the geometry of the induced fracture and the pressure history during the tests. Geophysical observations indicate heterogeneous distributions of rock properties around borehole SB3 (e.g., strength and/or elastic modulus variations due to pre-existing discontinuities in the rock mass), and it is known the rock is anisotropic. This might contribute to the discrepancy between the plane of the induced microseismicity and the current best estimate of the minimum principal stress orientation. It is planned to include the effect of heterogeneity and anisotropy in future simulations of on-going experiments at the GTS site which entail fault stimulation and hydraulic fracturing with larger injected volumes.

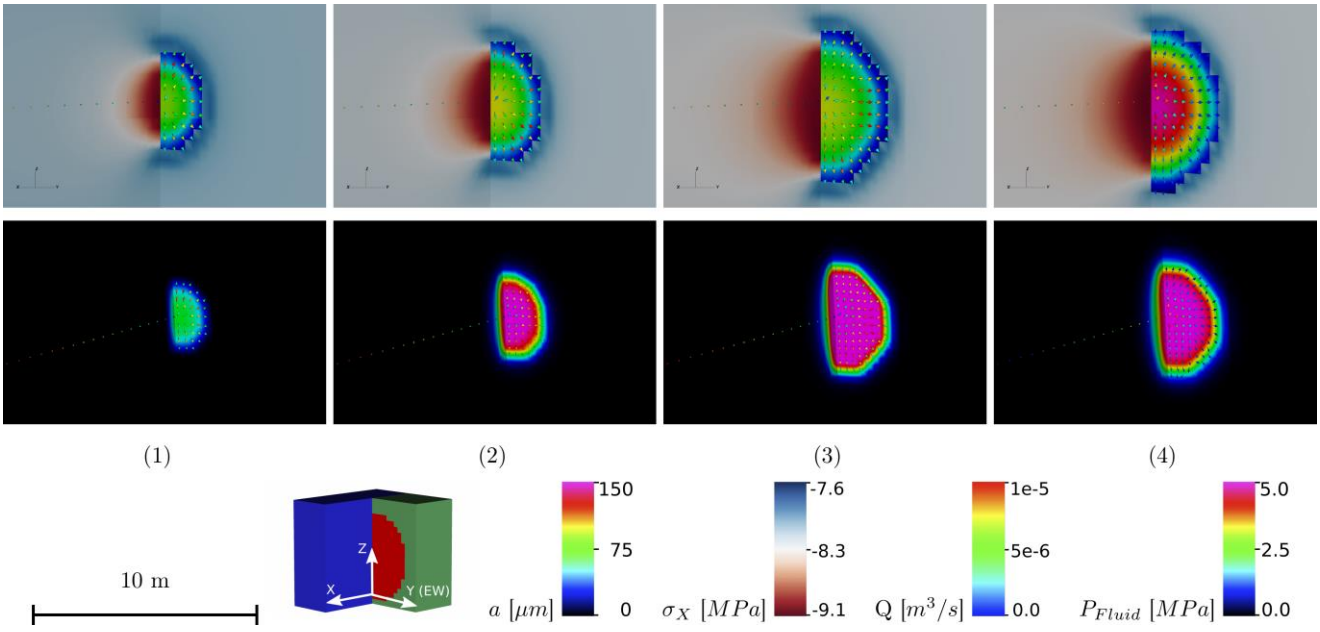

Figure 4: SB3-8 before shut-in during injection cycles 1-4 (left to right). The frames at top show the distributions of fracture aperture, a, minimum principal σ_x and flow rate vectors prevailing immediately before shut-in. The frames at bottom show the corresponding distributions of fluid pressure and flow rate vectors at the fracture-rock interface. The wellbore, going from the left of the Figure to the fracture center, is shown as a dotted line in all plots. A sketch illustrating the perspective view of the rock mass (blue and green) and fracture (red) is shown at the bottom.

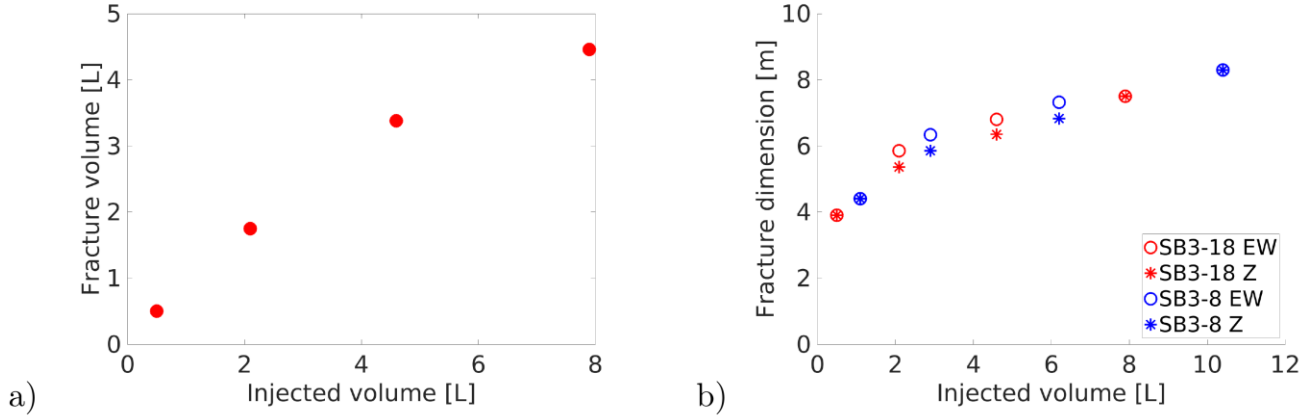

Figure 5: Simulated fracture dimensions: a) Fracture volume vs total injected volume in SB3-18; b) Fracture dimensions vs total injected volume in East-West (EW) and Z-direction.

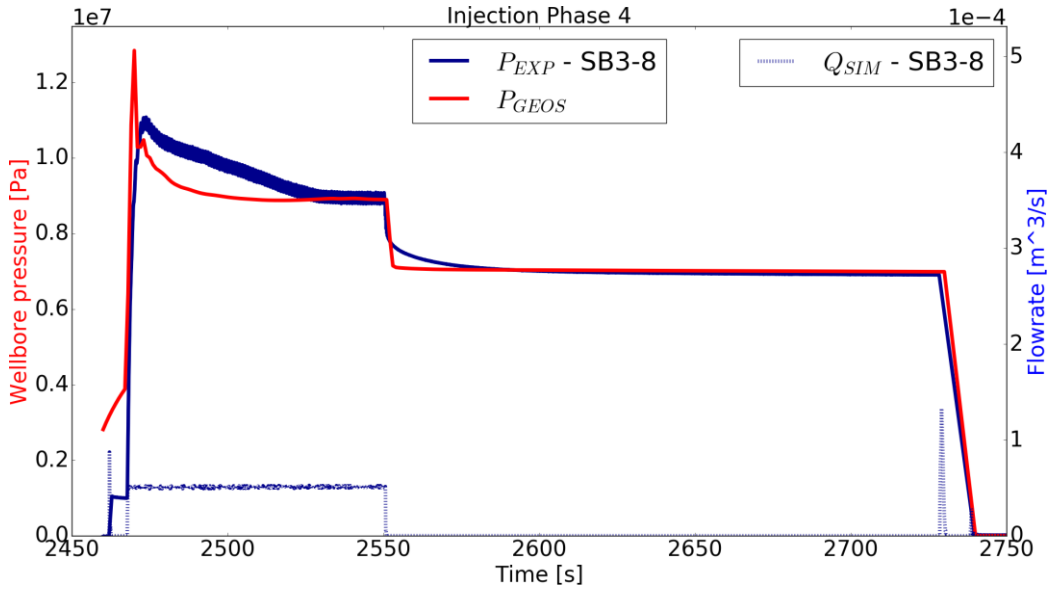

Figure 6: SB3-8. Injection flow rate and resulting pressure at wellbore head during injection cycle 4 for experiment and simulation.

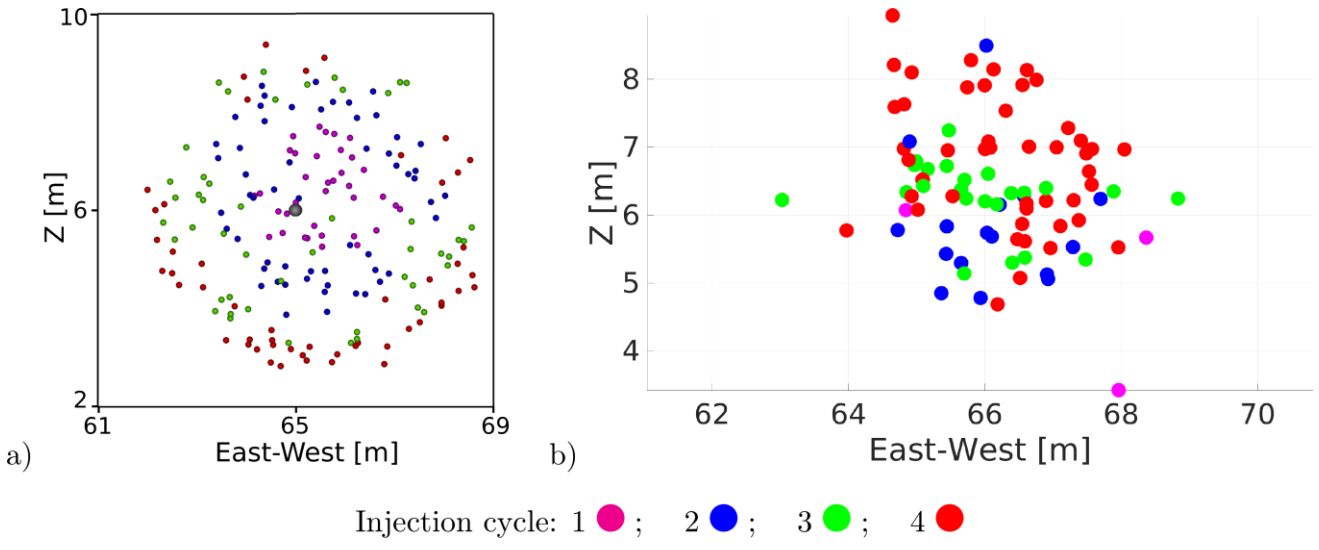

Figure 7: SB3-18. Microseismic activity in simulations (left) and experiments (right) viewed normal to the fracture (horizontal view from the north). Microseismic events are colored according to the injection cycles 1-4.

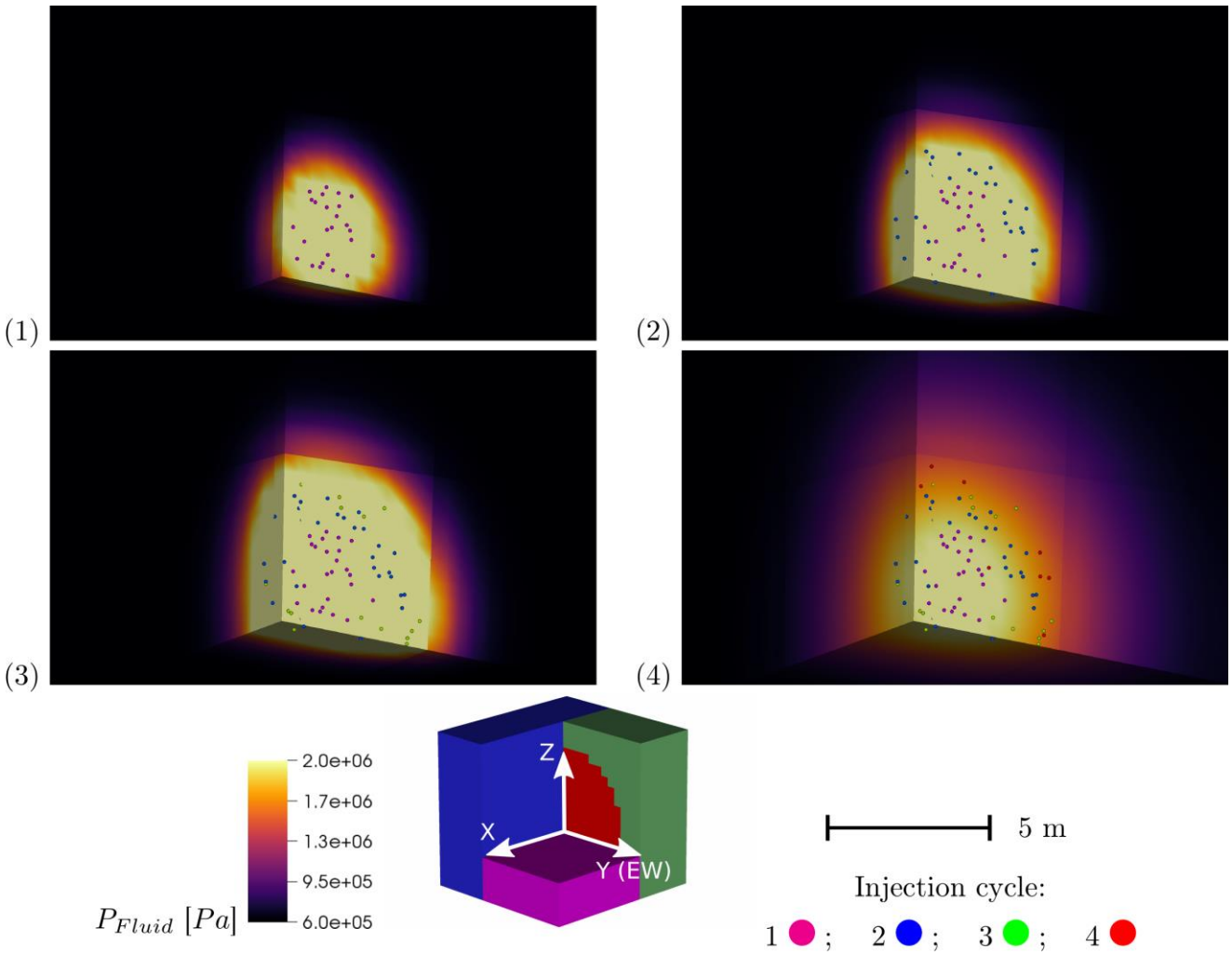

Figure 8: SB3-18. Snapshots of simulated microseismic activity and the fluid pressure distribution around the propagating fracture (fracture is not explicitly shown) at the end of the four injection cycles (i.e. immediately before the start of the subsequent injection cycle). Only one octant is shown, as illustrated by the sketch of the fracture region (red) within the rock mass (blue, green and magenta) shown at the bottom. The simulated microseismic events are colored according to the injection cycles 1-4.

CONCLUSIONS

Numerical simulations were made of hydraulic fracture stress tests conducted in the Deep Geothermal Underground Laboratory (DUG Lab) at the Grimsel Test Site, Switzerland. The simulations sought to reproduce the pressure response, hydraulic fracture dimensions and microseismic event distributions observed during the tests.

Model simulations for fracture dimensions yield a fracture diameter of roughly 7.5 m (SB3-18) and 8.3 m (SB3-8), which is in good agreement with fracture dimensions estimated from microseismic event distributions observed during the experiment. Microseismic events in the experiments predominantly occurred during the refracturing cycles, while seismic activity in the numerical simulations was more evenly distributed across all injection cycles. The pressure response during fracture propagation is captured in the numerical model, where an analytical wellbore solver is needed to reproduce post shut-in behavior. Microseismic events observed during the experiments defined planar structures that were not oriented perpendicular to the estimated orientation of the minimum stress, as would be expected were they to define classical hydrofractures. Whether this reflects structural control of the microseismic plane (i.e. activation in shear of a preexisting structure), local deviation of the minimum stress orientation from that estimated or both is currently uncertain. Simulation of the effect of the injections in a medium with pre-existing structures and foliation will be examined in future work.

The simulations reported in this paper can serve as a baseline for more complex models that will be applied to modeling on-going field experiments which entail fault stimulation and hydraulic fracturing with larger injected volumes.

ACKNOWLEDGEMENTS

The authors want to thank the NAGRA and the Grimsel Test Site, Switzerland. Funding by the Swiss Competence Center for Energy Research (SCCER) is gratefully acknowledged.

REFERENCES

Annavarapu, C., Settgast, R., Johnson, S., Fu, P. & Herbold, E. (2015), 'A weighted nitsche stabilized method for small-sliding contact on frictional surfaces', Computer Methods in Applied Mechanics and Engineering 283, 763 – 781.

Deichmann, N., Kraft, T. & Evans, K. (2014), 'Identification of faults activated during the stimulation of the basel geothermal project from cluster analysis and focal mechanisms of the larger magnitude events', Geothermics 52, 84 – 97.

Detournay, E. (2016), 'Mechanics of hydraulic fractures', Annual Review of Fluid Mechanics 48, 311–339.

Economides, M. et al. (2000), Reservoir stimulation, Vol. 18.

Evans, K. (2005a), 'Permeability creation and damage due to massive fluid injections into granite at 3.5 km at soultz: 2. critical stress and fracture strength', Journal of Geophysical Research: Solid Earth 110(B4).

Evans, K. F. , Moriya, H., Niitsuma, H., Jones, R. H., Phillips, W. S., Genter, A., Sausse, J., Jung, R., Baria, R. (2005b) Microseismicity and permeability enhancement of hydrogeologic structures during massive fluid injections into granite at 3 km depth at the Soultz HDR site. *Geophys J Int* 2005; 160 (1):

Evans, K., Cornet, F., Hashida, T., Hayashi, K., Ito, T., Matsuki, K. & Wallroth, T. (1999), 'Stress and rock mechanics issues of relevance to hdr/hwr engineered geothermal systems: review of developments during the past 15 years', Geothermics 28(4–5), 455 – 474.

Fu, P., Cruz, L., Moos, D., Settgast, R. & Ryerson, F. (2015), Numerical investigation of a hydraulic fracture bypassing a natural fracture in 3d, in '49th US Rock Mechanics Symposium', ARMA, San Francisco, California.

Fu, P., Hao, Y., Walsh, S. & Carrigan, C. (2016), 'Thermal drawdown-induced flow channeling in fractured geothermal reservoirs', Rock Mechanics and Rock Engineering 49(3), 1001–1024.

Gischig, V., Doetsch, J., Krietsch, H., Maurer, H., Amann, F., Evans, K., Jalali, M., Obermann, A., Nejati, M., Valley, B., Wiemer, S. & Giardini, D. (2017), 'On the link between stress field and small-scale hydraulic fracture growth in anisotropic rock derived from micro-seismicity', in preparation.

Gischig, V. & Wiemer, S. (2013), 'A stochastic model for induced seismicity based on non-linear pressure diffusion and irreversible permeability enhancement', Geophysical Journal International.

Guo, B., Fu, P., Hao, Y., Peters, C. & Carrigan, C. (2016), 'Thermal drawdown-induced flow channeling in a single fracture in egs', Geothermics 61, 46–62.

Keusen, H., Ganguin, J., Schuler, P. & Buletti, M. (1989), 'Grimsel test site: Geology rep., nationale genossenschaft fuer die lagerung radioaktiver abfaelle (nagra)'.

Kim, W. (2013), 'Induced seismicity associated with fluid injection into a deep well in Youngstown, Ohio', J. Geophys. Res. Solid Earth 118, 3506–3518.

Konietzky, H. (1995), 'Versuch excavation disturbed zone 3d stress field and 2d disturbed zone modelling for the grimsel test siterep., internal report 95-62. wettingen: Nagra.'.

Kraft, T. & Deichmann, N. (2014), 'High-precision relocation and focal mechanism of the injection-induced seismicity at the Basel EGS', Geothermics 52, 59–73.

Niitsuma, H., Fehler, M., Jones, R. H., Wilson, S., Albright, J., Green, A., Baria, R., Hayashi, K., Kaida, H., Tezuka, K. Jupe, A., Wallroth, T., Cornet, F., Asanuma, H., Moriya, H., Nagano, K., Phillips, S.S., Rutledge, J., House, L., Beauce, A., Alde, D., and Aster R. (1999), Current status of seismic and borehole measurements for HDR/HWR development, *Geothermics, 29*, 475-490.

McClure, M. & Horne, R. (2014a), 'Correlations between formation properties and induced seismicity during high pressure injection into granitic rock', Engineering Geology 175, 74 – 80.

McClure, M. & Horne, R. (2014b), 'An investigation of stimulation mechanisms in enhanced geothermal systems', International Journal of Rock Mechanics and Mining Sciences 72, 242 – 260.

Pahl, A., Heusermann, S., Brauer, V. & Gloeggler, W. (1989), 'Grimsel test site. rock stress investigations, Hannover, Germany: Bgr-nagra rep. ntb'.

Settgast, R., Fu, P., Walsh, S., White, J., Annavarapu, C. & Ryerson, F. (2016), 'A fully coupled method for massively parallel simulation of hydraulically driven fractures in 3-dimensions', International Journal for Numerical and Analytical Methods in Geomechanics.

Settgast, R.R., Johnson, S., Fu, P. & Walsh, S.D.C. (2014), Simulation of hydraulic fracture networks in three dimensions utilizing massively parallel computing resources. Unconventional Resources Technology Conference (URTEC), 2014.

Settgast, R., Johnson, S., Fu, P., Walsh, S. & Ryerson, F. (2012), Simulation of hydraulic fracture networks in three dimensions, in 'Stanford Geothermal Workshop', Stanford University Press, Palo Alto.

Sherman, C., Templeton, D., Morris, J. & Matzel, E. (2016), Modeling induced microseismicity in an enhanced geothermal reservoir, in '50th US Rock Mechanics Symposium', ARMA, Houston, TX.

Tester, J., Anderson, B., Batchelor, A., Blackwell, D., DiPippo, R., Drake, E., Garnish, J., Livesay, B., Moore, M., Nichols, K. et al. (2006), 'The future of geothermal energy: Impact of enhanced geothermal systems (egs) on the united states in the 21st century', Massachusetts Institute of Technology 209.

Vogler, D., Settgast, R.R., Annavarapu, C., Bayer, P., Amann, F. (2016a), Hydro-mechanically coupled flow through heterogeneous fractures, in 'Stanford Geothermal Workshop', Stanford University Press, Palo Alto.

Vogler, D., Amann, F., Bayer, P. & Elsworth, D. (2016b), 'Permeability evolution in natural fractures subject to cyclic loading and gouge formation', Rock Mechanics and Rock Engineering pp. 1–17.

Walsh, S. & Carroll, S. (2013), 'Fracture-scale model of immiscible fluid flow', Physical Review E 87(1), 013012.

Walsh, S., Du Frane, W., Mason, H. & Carroll, S. (2013), 'Permeability of Wellbore-Cement Fractures Following Degradation by Carbonated Brine', Rock Mechanics and Rock Engineering 46(3), 455–464.

Walsh, S., Settgast, R. & Johnson, S. (2012), A laboratory and numerical study of chemo-mechanically mediated permeability evolution in the near-wellbore region, in '46th Meeting of the American Rock Mechanics Association', ARMA, Chicago.

Wolhart, S., Harting, T., Dahlem, J., Young, T., Mayerhofer, M., Lolon, E. et al. (2006), Hydraulic fracture diagnostics used to optimize development in the jonah field, in 'SPE Annual Technical Conference and Exhibition', Society of Petroleum Engineers.